Journal of Engineering Research

Volume 7 | Issue 2 Article 34

2023

Behavior of Hexagonal Concrete-Filled Double-Skin Steel Short Columns under the Effect of Axial Compression

Hend Adlan Selima

Journal of Engineering Research (ERJ)
Vol. 7 – No. 2, 2023
©Tanta University, Faculty of Engineering
ISSN: 2356-9441 https://erjeng.journals.ekb.eg/ e ISSN: 2735-4873

Behavior of Hexagonal Concrete-Filled Double-Skin Steel Short Columns under the Effect of Axial Compression

Hend Ramadan[1], Mostafa Hassanein[2], Yousry Bayoumy Shaheen[3]

[1] Teaching Assistant, Civil Engineering Department, Higher Institute of Engineering and Technology in Kafr El sheikh, Egypt
[2] Professor of Steel Structures and Bridges, Civil Engineering Department, Faculty of Engineering, Tanta University, Egypt
[3] Professor of Strength and Testing of Materials, Civil Engineering Department, Faculty of Engineering, Menoufia University, Egypt
email: hend.selima@kfs-hiet.edu.eg, Hassanein@f-eng.tanta.edu.eg, yousry shaheen@sh-eng.menofia.edu.eg

***Abstract*-Concrete-filled double skin tubular (CFDST) columns involve a tube-in-tube arrangement, where the steel sections can be round, square or rectangular hollow sections, with the annulus between the hollow sections filled with concrete. To date, there have been no significant applications of hexagonal concrete-filled double skin tubular columns (HCFDST) that have inner tubes with circular hollow section (CHS) and outer tubes with hexagonal hollow section (HHS) worldwide, partly due to the lack of design provisions. To obtain the structural behavior of HCFDST columns, a finite element (FE) analysis was conducted. To indicate the accuracy and the reliability of the model, the proposed FE model was verified by the available experimental data for HCFDST. Columns were employed to conduct parametric studies. The effects of various parameters on the load-displacement response of HCFDST short columns were studied by using the validated FE model. A new formula to determine ultimate load for regular HCFDST short columns in compression has been proposed in this study.**

***Keywords*-Concrete-filled steel tubes, Finite element analysis, Ultimate strength, Short columns and HCFDST.**

I. INTRODUCTION

The load of the construction was transferred to the foundation using columns. Composite columns are an illustration of how systems that incorporate the interaction of structural steel components with concrete can be used effectively. The first use of composite columns was to meet the steel section's fire rating criteria. Steel tubes filled with concrete make up the composite members known as concrete-filled steel tubular (CFST) columns. CFST columns have a number of benefits. High-rise constructions and long span structures both use columns [1, 2]. The strength of columns was enhanced by using ferrocement as a reinforcing approach [3]. For functionality in many industries, the desired material must be both robust and light weight, while economic considerations demand properties like cheap cost and ease of fabrication. As a result, the usage of concrete filled double skin tubular (CFDST) columns, which are made up of two roughly equidistant tubes with concrete filling the gap in between, has been reinstated.

Fig. 1. shows most typical cross sections of the CFDST. Because of the hollow inner voids, CFDSTs columns are lighter-weight columns [4–8]. The CFDST cross-section concept initially appeared in pressure vessel submerged tube tunnels [9]. When compared to the traditional CFST columns, the CFDST columns are stronger and more flexible [10–13]. The confinement effect created by the hollow steel tubes is responsible for the increased ductility and yield strength. In order to lighten the weight of the structure while keeping a high energy absorption capacity against seismic loading, CFDSTs columns have also been deployed in Japan as high-rise bridge piers [14].

Recently, high rise buildings have been constructed using hexagonal CFDST (HCFDST) members, which function as enormous columns in the mega frame-core tube systems [15, 16] depicted in Fig.3. (a and b). The maximum load capacity and ductility of hexagonal steel tubes are higher than those of square ones [17]. The dual-axisymmetric hexagonal column design with four interior angles of 135° and two interior angles of 90° in the opposite directions has a lower load carrying capability than the normal shape with a 120° internal angle [18].

For the estimation of the ultimate load capacity for circular and regular polygonal CFST columns, Yu et al. [19] proposed a design equation. For typical hexagonal concrete-filled steel tubes (HCFSTs). Evirgen et al. [20] conducted experiments to examine the impact of the width/thickness ratio (b/t) on ultimate strengths, ductility, and buckling behavior.

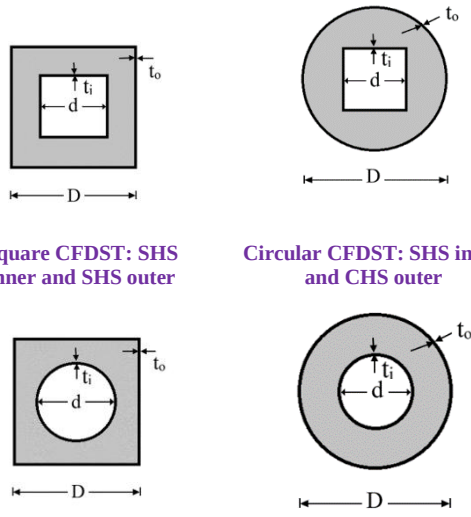

Square CFDST: SHS inner and SHS outer | Circular CFDST: SHS inner and CHS outer

Square CFDST: CHS inner and SHS outer | Circular CFDST: CHS inner and CHS outer

Figure 1. Types of CFDST column cross-sections.

DOI: 10.21608/ERJENG.2023.201459.1168

Journal of Engineering Research (ERJ)
Vol. 7 – No. 2, 2023
©Tanta University, Faculty of Engineering
ISSN: 2356-9441 https://erjeng.journals.ekb.eg/ e ISSN: 2735-4873

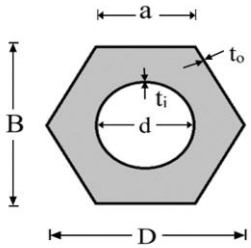

Figure 2. Hexagonal CFDST: CHS inner and HHS outer.

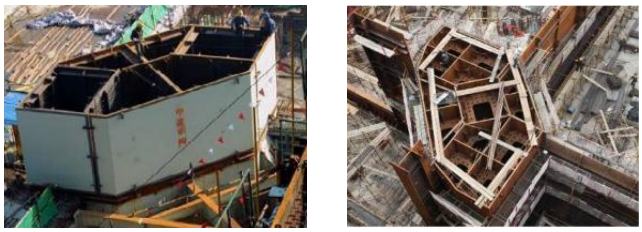

(a) Gaoyin finance building (h=597 m) **(b) Z15 tower (h = 528 m)**

Figure 3. Hexagonal CFST members applications in high-rise buildings.

The mechanical performance of HCFST columns was the subject of experimental investigation by Xu et al. [15], and also suggested a formula for computing the ultimate compressive and flexural strength. Eight HCFST columns were evaluated under compression loading by Ding et al. [21], and also suggested a design equation for maximum strength of the HCFST stub columns. In order to forecast the ultimate axial strength of hexagonal concrete-filled steel tubular short columns, Hassanein et al. [18] proposed a novel design equation. Seven specimens of stiffened HCFDST stub columns were evaluated by Shen et al. [22] under an axial load, and gave improved formulas based on the equations suggested by MOHURD 2014 [23]. Only two of the seven examples in the prior study [23] were HCFDST columns; the remaining five specimens were HCFDST columns with ribs and strips. As a result, this work provided a thorough analysis of HCFDST columns. In order to calculate the ultimate load for standard HCFDST short columns in compression, this study developed a new formula. The new proposed formula's average and coefficient of variation (COV) showed good agreement with the Shen et al.'s equation [23].

The compressive behavior of HCFDST stub columns was the subject of this study. Under compression, a total of 24 specimens were tested with various parameters. Finally, calculations based on the yielding strengths of the tubes and the strength of the filled concrete were provided to estimate their strengths under compression.

II. FINITE ELEMENT MODELLING

A. General

Short HCFDST columns with inner circular tubes were simulated and their behavior was examined using the finite element program ABAQUS [24]. The choice of element type, mesh size, boundary conditions, and load application all affect the ability of FE models to accurately represent the definition of materials and the interface between concrete and steel tubes. To evenly transfer the load on the steel tubes and the sandwiched concrete, two endplates were employed to cover both ends of the HCFDST short column. One of the end plates was fixed to the bottom of the HCFDST while the other one was placed to its top.

B. Boundary Condition and Load Application

All degrees of freedom for the top and bottom surfaces of columns were restricted, with the exception of the top surface's displacement in the direction of the applied load at the loaded end. The load was applied using the ABAQUS STATIC option. Utilizing the modified RIKS method included in the ABAQUS library, the load was applied in small increments. To impart a consistent load to the top surface of the upper plate, the load was determined using the PRESSURE option.

C. Finite Element Type and Mesh

According to Elchalakani et al. [25], the steel tubes, end plates, and concrete in the HCFDST construction were modelled using three-dimensional 8-Node solid elements (C3D8R) linear brick with decreased integration, linear geometric order, and hexahedron element form. Both the effective mesh at contact surfaces and the deflected shape of steel tubes are captured by the solid element (C3D8R) [26–28]. The steel tubes and concrete infill had a 17 mm HCFDST estimated global mesh size. The finite element mesh for HCFDST columns is shown in Figure 4.

D. Interactions

Surface interaction properties are created using the SURFACE INTERACTION option in ABAQUS. Contact interactions are governed by surface interaction characteristics. The primary need is the friction between the two sides, which is preserved for as long as the surfaces were in contact.

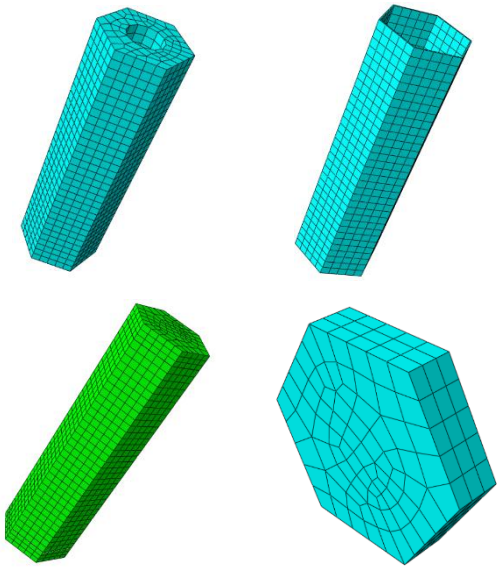

Figure 4. Finite element mesh for HCFDST columns.

DOI: 10.21608/ERJENG.2023.201459.1168

Journal of Engineering Research (ERJ)
Vol. 7 – No. 2, 2023
©Tanta University, Faculty of Engineering
ISSN: 2356-9441 https://erjeng.journals.ekb.eg/ e ISSN: 2735-4873

While the tie constraint was employed between the endplates and HCFDST, surface-to-surface contact was chosen to simulate the interaction between the steel tubes and concrete. "Hard contact" is the interaction of two deformable surfaces in the normal direction that characterizes "normal behavior". As a result, there is no compression penetration between the surfaces, allowing for tension separation following contact. The friction coefficient (μ) of 0.3, as proposed by Pagoulatou et al. [29], defines the tangential features of the contact surface.

E. Material Modelling Steel

The elastic modulus (Es) and Poisson's ratio for steel were chosen as 200 GPa and 0.3, respectively, to create the material model for the specimen. Figure 5 displays the elastoplastic stress-strain curve for steel from Anumolu et al. [30].

F. Confined sandwich concrete material

The Ding et al. [21] modified model was used to simulate the compressive behavior of sandwich concrete. The stress-strain curve for sandwich concrete is depicted in Fig. 6. The behavior of confined concrete under compression was simulated using the concrete damaged-plasticity model. The concrete model under tri-axial compression presented by Ottosen [31] was updated by Ding et al. [21] and utilized to study the axial behavior of HCFDSTs. The stress-strain relationship is discussed in (1):

$$y = \begin{cases} \frac{kx+(m-1)x^2}{1+(k-2)x+mx^2} & x \le 1 \\ \frac{x}{\alpha_1(x-1)^2+x} & x > 1 \end{cases} \quad (1)$$

In which f_c =0.4 $f_{cu}^{7/6}$is the uniaxial compressive strength of concrete, f_{cu} is the compressive cubic strength of concrete, and ε_c = 383 $f_{cu}^{7/18}$×10 -6 is the strain corresponding with the peak compressive stress of concrete. $y = \sigma/f_c$ and x = $\varepsilon/\varepsilon_c$ are the stress and strain ratios of the core concrete to the uniaxial compressive concrete, respectively. The ratio of the initial tangent modulus to the secant modulus at peak stress is the parameter k, m=1.6 $(k\text{-}1)^2$ is a parameter that governs the reduction in the elastic modulus along the ascending branch of the axial stress-strain relationship, E_c = initial modulus of elasticity equal to 4700 $\sqrt{f_c}$ according to the ACI 2014 [32] and Poisson's ratio = 0.2.

According to Bazant et al. [33], the fracture energy Gf can be computed in (2) and the tensile strength f_t can be assumed to equal 10% of the uniaxial compressive strength. (2). The maximum coarse aggregate size for this investigation is 15 mm.

$$G_f = (0.049d_{max}^2 - 0.5d_{max} + 26)(0.1f_c)^{0.7} \ N/m \quad (2)$$

III. VALIDATION OF THE DEVELOPED FINITE ELEMENT

The validity of the FE modelling approach utilized here was evaluated using the test results from two studies conducted by Shen et al. [22] and Ding et al. [21].

Seven specimens in all are created and tested by Shen et al. [22], including two HCFDST columns, two hexagonal multicavity CFDST (HMCFDST) columns which consist of strips divide the section into multiple closed cavities, and three S-HMCFDST columns which can be stiffened by ribs, as shown in Fig. 7. The descriptions of the specimens are shown in Table 1. where h_s and h_s = width of rib and strip, respectively. The material characteristics of steel tubes are shown in Table 2.

The numerical ultimate strengths $N_{ul,FE}$ obtained by the models are compared with results of experiments N_{Exp} performed by Shen et al. [22] in Table 3.

Table 3 also includes statistical parameters for the numerical to test ratio $N_{ul,FE}$ /N_{Exp}, including mean, standard deviation (SD), and coefficient of variation. (COV). With a mean value of 1.035, which is on the safe side and close to the unity baseline, 0.059 standard deviation (SD), and 0.058 coefficient of variation (COV), which are low values that reflect its reliability. The results demonstrate the accuracy of the modelling strategy proposed herein for specimens in compression. Figure 8 illustrates the load-axial displacement relationships for the columns considering the experimental and FE results. Ding et al. [21] tested a total of 8 hexagonal CFST specimens. The specifications of the specimens are shown in Table 4. where B is the length of outer edge of the hexagonal section, (L) is the specimen length and (t) is the steel tube thickness.

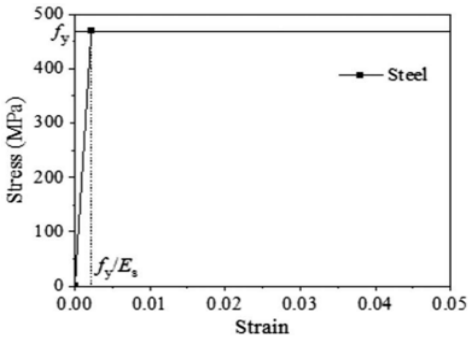

Figure 5. Stress-strain curve for steel.

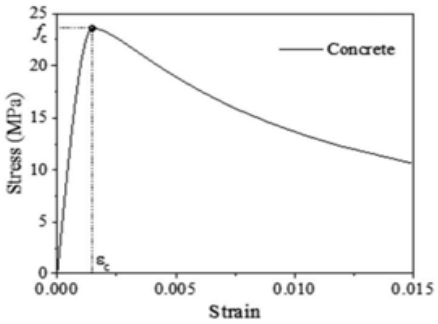

Figure 6. Stress vs. strain curve for concrete

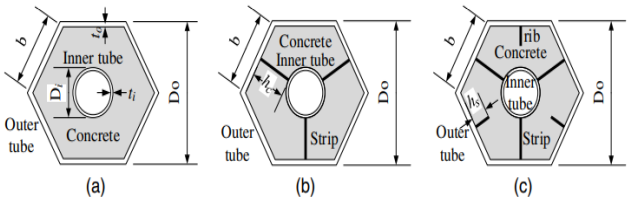

Figure 7. Cross section of test members: (a) HCFDST; (b) HMCFDST; (c) S-HMCFDST.

Journal of Engineering Research (ERJ)
Vol. 7 – No. 2, 2023
©Tanta University, Faculty of Engineering
https://erjeng.journals.ekb.eg/
ISSN: 2356-9441
e ISSN: 2735-4873

Table 1. Details of specimens

Specimen	b (mm)	D_o (mm)	t_o (mm)	di (mm)	t_i (mm)	h_c (mm)	h_s (mm)
H-L	169.74	300	2.73	114	4.02	0	0
H-H	169.74	300	2.73	180	5.09	0	0
H-L-P00	169.74	300	2.73	114	4.02	90	0
H-H-P00	169.74	300	2.73	180	5.09	57	0
H-L-P30	169.74	300	2.73	114	4.02	90	30
H-L-P57	169.74	300	2.73	114	4.02	90	57
H-H-P30	169.74	300	2.73	180	5.09	57	30

Table 2. Material properties of steel tubes

Material	Element	Inner tube diameter (mm)	Thickness (mm)	E_s (GPa)	f_y (MPa)	f_u (MPa)
Q355 plate	Hexagonal tube	0	2.73	212.1	483.7	605.2
	Strip	0	2.73	191.9	484.8	589
	Rib	0	2.73	212.6	468.3	590.1
Seamless steel tube	Inner tube	114	4.02	191.7	437.3	615.8
		180	5.09	185.4	375.5	622.8

Table 3. Ultimate strengths of axially loaded hexagonal CFDST short columns

Specimen	N_{Exp}	$N_{ul,F.E}$	$N_{ul,F.E}$ / N_{Exp}
H-L	3405.5	3490	1.025
H-H	2975.3	3380	1.136
H-L-P00	4160.7	3878	0.932
H-H-P00	3573.3	3779	1.058
H-L-P30	3931.3	4085	1.039
H-L-P57	4145.3	4240	1.023
H-H-P30	3855.5	3980	1.032
Mean			1.035
SD			0.059
COV			0.058

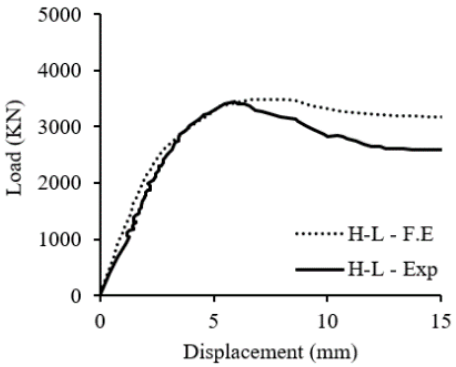

(a) H-L

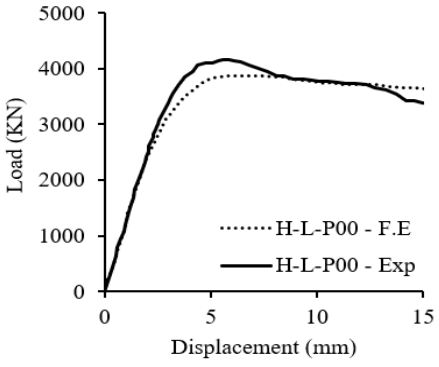

(b) H-L-P00

DOI: 10.21608/ERJENG.2023.201459.1168

Journal of Engineering Research (ERJ)
Vol. 7 – No. 2, 2023
©Tanta University, Faculty of Engineering
ISSN: 2356-9441 https://erjeng.journals.ekb.eg/ e ISSN: 2735-4873

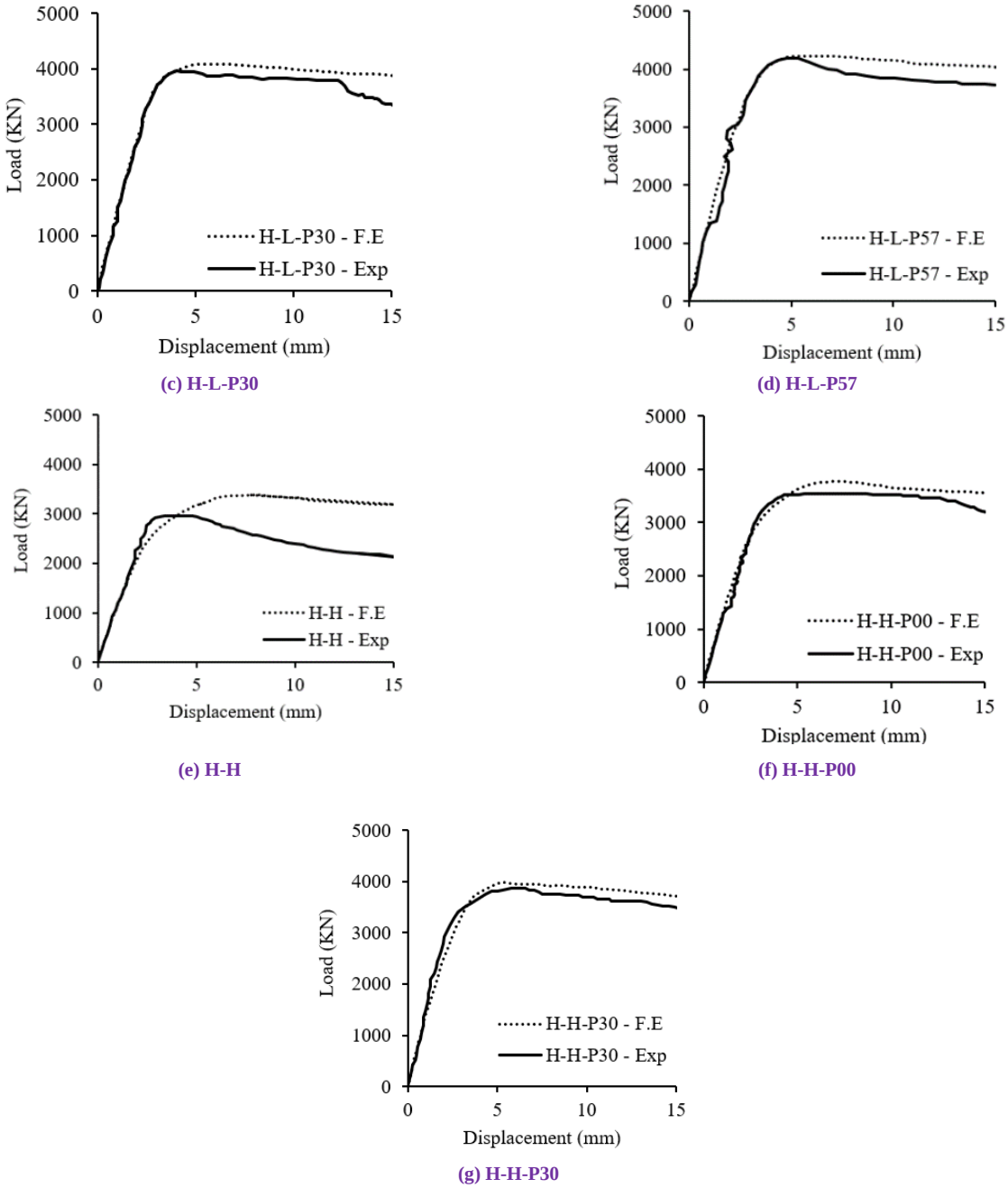

(c) H-L-P30 (d) H-L-P57

(e) H-H (f) H-H-P00

(g) H-H-P30

Figure 8. Comparison between FE modelling and experimental results for load-displacement curves of specimens: (a) H-L; (b) H-L-P00; (c) H-L-P30; (d) H-L-P57; (e) H-H; (f) H-H-P00 and (g) H-H-P30.

Table 4. Details of specimens and ultimate strengths of axially loaded hexagonal CFST short columns.

Specimen	$B \times t$ (mm×mm)	L (mm)	f_c (MPa)	f_y (MPa)	f_u (MPa)	E_s (GPa)	$N_{ul,F.E}$ (kN)	$N_{ul,F.E}$ (kN)	$N_{ul,F.E}$ / N_{Exp}
HST1-A	196 × 3.73	1200	32.24	311	460	209	4947	4809	0.972
HST1-B	198 × 3.71	1200	32.24	311	460	209	4618	4809	1.041
HST2-A	196 × 5.78	1200	32.24	321	480	202	6001	5703	0.950
HST2-B	198 × 5.96	1200	32.24	321	480	202	6041	5703	0.944
HST3-A	197 × 3.72	1200	48.98	311	460	209	6827	6432	0.942
HST3-B	198 × 3.76	1200	48.98	311	460	209	6803	6432	0.945
HST4-A	199 × 5.89	1200	48.98	321	480	202	7079	6988	0.987
HST4-B	196 × 5.81	1200	48.98	321	480	202	7289	6988	0.959
Mean									0.9675
SD									0.0336
COV									0.0347

DOI: 10.21608/ERJENG.2023.201459.1168

Journal of Engineering Research (ERJ)
Vol. 7 – No. 2, 2023
©Tanta University, Faculty of Engineering
ISSN: 2356-9441 https://erjeng.journals.ekb.eg/ e ISSN: 2735-4873

Table 4 includes the numerical to test ratio $N_{ul,FE}$ /N_{Exp} and statistical parameters associated with this ratio including mean, standard deviation (SD), and coefficient of variation (COV). The numerical ultimate strengths $N_{ul,FE}$ are compared against test results N_{Exp} carried out by Ding et al. [21]. According to the results, a mean value of 0.977, 0.0336 standard deviation (SD) and 0.0347 coefficient of variation (COV) which are small values that shown its reliability.

Figure 9 presents the load-axial displacement relationships for the columns taking into consideration the FE and experimental results.

IV. PARAMETRIC STUDY

Two steel materials with yield strengths (f_y) of 250 and 350 MPa and 40 MPa of concrete compressive strength (f_c) are included in the parametric analysis. Table 5 displays the results.

A total of 24 numerical models produced, including 12 fundamental geometries. The models are first subdivided into two groups (G1-1 and G1-2) based on their steel yield strength f_y before remaining in one group G1 with a concrete strength value of f_c = 40 MPa.

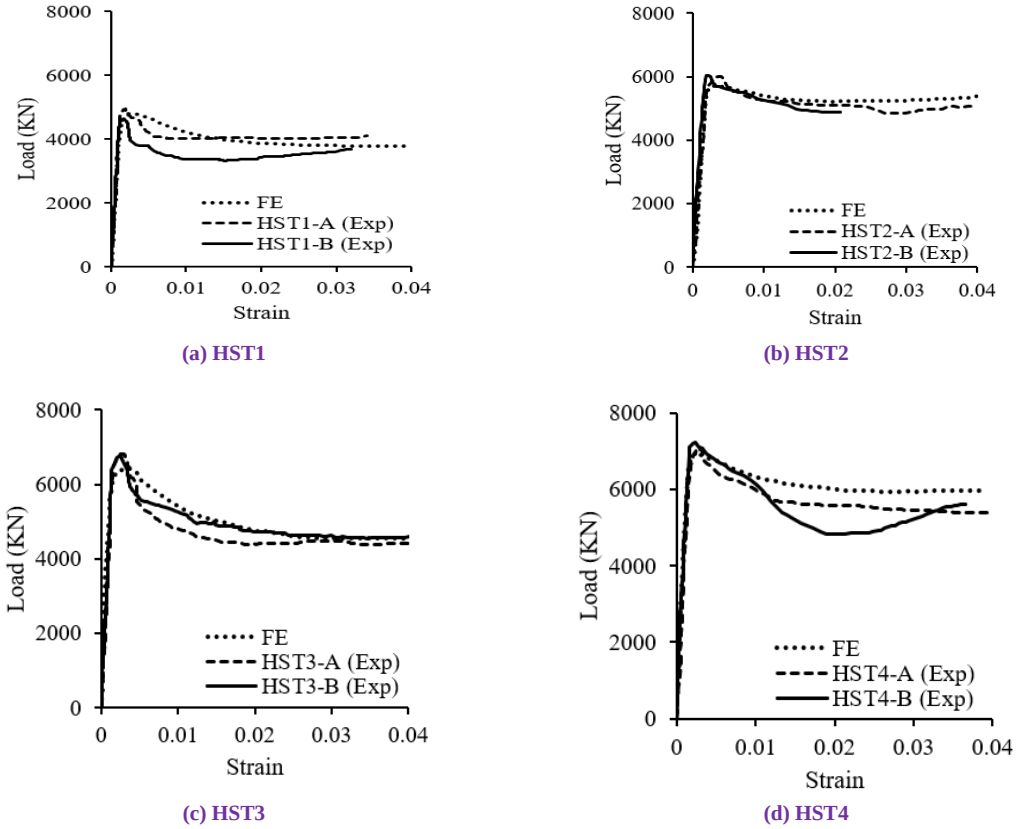

(a) HST1 (b) HST2

(c) HST3 (d) HST4

Figure 9. Comparison between FE modeling and experimental results for load-displacement curves of specimens: (a) HST1; (b) HST2; (c) HST3; (d) HST4.

Table 5. Details and ultimate strengths of the FE model of HCFDST short column with fc = 40 MPa - G1

Outer tube dimensions				Inner tube dimensions			Hollow ratio	G1-1: f_y =250 (MPa)		G1-2: f_y =350(MPa)	
D_o (mm)	B (mm)	t_o (mm)	D_o/t_o	d_i (mm)	t_i (mm)	d_i/t_i	χ	No	$N_{ul,F.E}$ (kN)	No	$N_{ul,F.E}$ (kN)
150	130	2	75	60	3	20	0.48	A1	787	A13	943
		2	75	60	5	12	0.48	A2	905	A14	1098
		4	37.5	70	3	23	0.57	A3	986	A15	1269
		4	37.5	70	5	14	0.57	A4	1132	A16	1502
200	173	2	100	70	3	23	0.41	A5	1370	A17	1504
		2	100	70	5	14	0.41	A6	1523	A18	1632
		4	50	100	5	20	0.61	A7	1636	A19	2109
		4	50	100	7	14	0.61	A8	1803	A20	2252
300	260	2	150	100	5	20	0.39	A9	2671	A21	2960
		2	150	100	7	14	0.39	A10	2736	A22	3208
		4	75	140	5	28	0.57	A11	2996	A23	3680
		4	75	140	7	20	0.57	A12	3205	A24	3912

DOI: 10.21608/ERJENG.2023.201459.1168

Journal of Engineering Research (ERJ)
Vol. 7 – No. 2, 2023
©Tanta University, Faculty of Engineering
ISSN: 2356-9441 https://erjeng.journals.ekb.eg/ e ISSN: 2735-4873

A. *Effect of Steel Yield Strengths*

Steel yield strengths between 250 and 350 MPa were used to analyze the behavior of HCFST specimens. The axial load-displacement curves for HCFDST specimens with various steel yield strengths are shown in Figure 10.

Although columns A1 and A13 in Fig. 10 (a) shown f_y values of 250 and 350 MPa, respectively, both had = 0.48. Figure 10 illustrates an increase in the ultimate strength by nearly 20% when the steel yield strength increased from 250 MPa to 350 MPa. (a).

Columns A3 and A15 of Figure 10 (b) are filled with steel yield strengths of 250 and 350 MPa, respectively, but both with = 0.57. Figure 10 shows that as the steel yield strength increased from 250 MPa to 350 MPa, the ultimate strength increased by about 29%. According to the results, strengthening the steel yield significantly enhances the ultimate strength of HCFDST short columns.

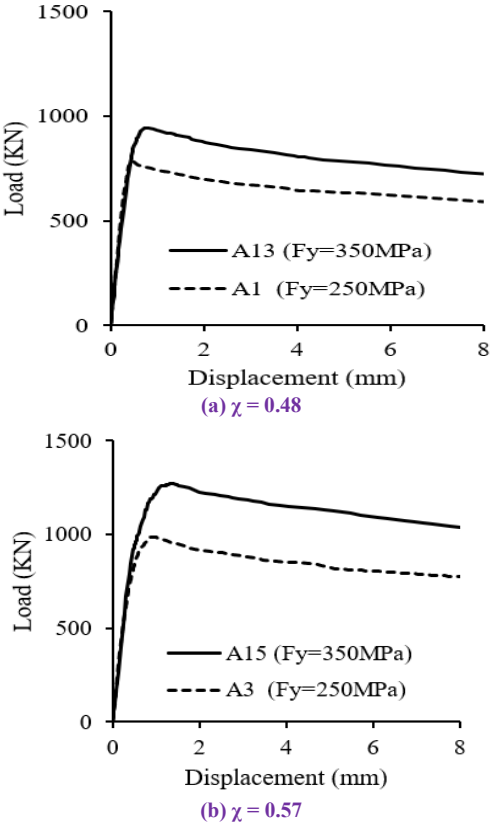

Figure 10. Load-displacement curves for HCFDST short columns showing the effect of steel fy value.

B. *Effect of Inner Tube Thickness*

The load displacement curves for HCFDST specimens with various inner tube thicknesses are shown in Figure 11. It can be shown that as inner tube thickness (t_i) grows while maintaining the same hollow ratio, the maximum load capacity improves. The ultimate strength only slightly improved, by around 17% and 8%, respectively, when the inner tube thickness was increased from 3 mm to 5 mm and from 5 to 7 mm.

C. *Effect of Hollow Ratio*

The axial load displacement curves for HCFDST specimens with various hollow ratios are shown in Figure 12. One important factor that influences the compressive behavior of the CFDST columns is the hollow ratio (χ), which is defined as $d_i/(D_o\text{-}2t_o)$.

The hollow ratio (χ) ranged between 0.48 and 0.57, 0.41 and 0.61, and (0.39 to 0.56). When the hollow ratio (χ) changed from (0.48 to 0.57), (0.41 to 0.61) and (0.39 to 0.56), respectively, the ultimate load capacity improved by approximately 25%, 18%, and 17%. To achieve this, the inner tube diameter and inner steel tube thickness were increased while the outer tube thickness and diameter remained constant.

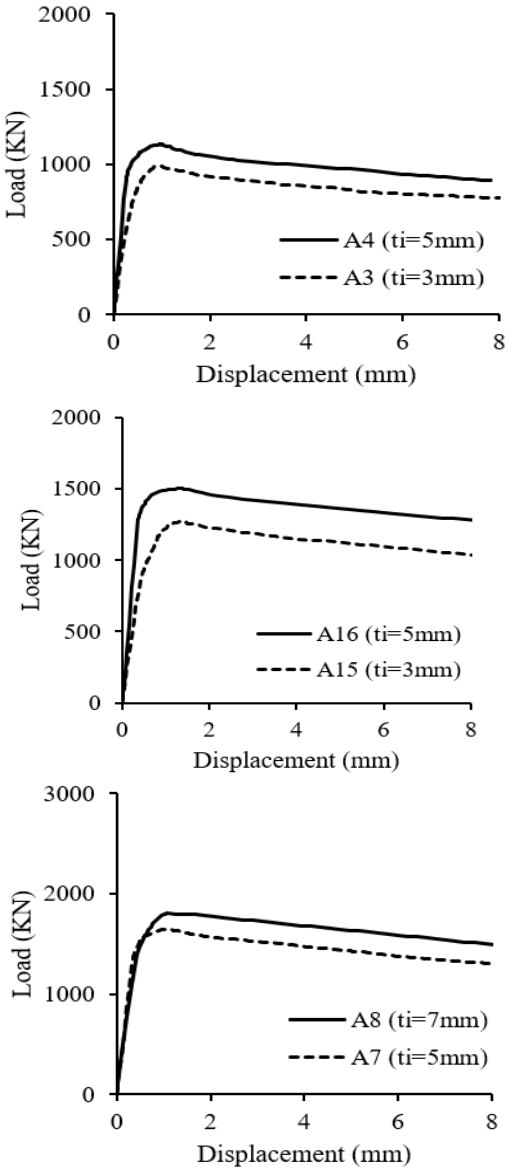

DOI: 10.21608/ERJENG.2023.201459.1168

Journal of Engineering Research (ERJ)
Vol. 7 – No. 2, 2023
©Tanta University, Faculty of Engineering
ISSN: 2356-9441 https://erjeng.journals.ekb.eg/ e ISSN: 2735-4873

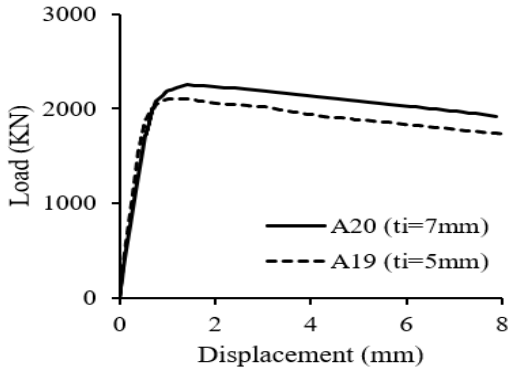

Figure 11. Load-displacement curves for HCFDST short columns showing the effect of the inner tube thickness (ti)

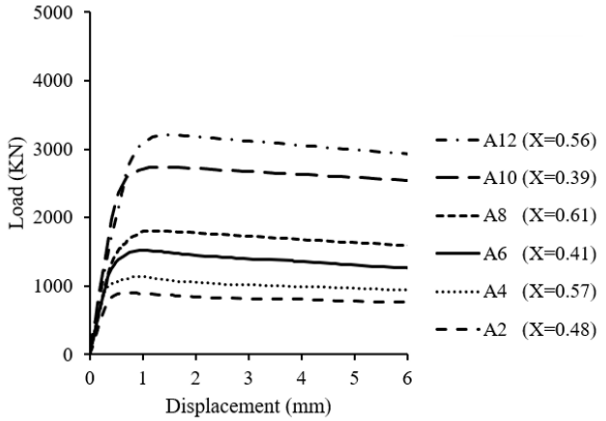

Figure 12. Load-displacement curves for HCFDST short columns showing the effect of hollow ratio (χ)

V. PROPOSED FORMULAE OF MAXIMUM LOAD STRENGTH CALCULATION

The maximum load strength of the HCFDST column can be calculated by:

$$N_P = f_{scy}A_{sc} + f_{yi}A_{si} \quad (3)$$

$$A_{sc} = A_{so} + A_c \quad (4)$$

where N_p = maximum load strength; f_{scy} = compound axial compressive stregth of the outer tube and the sandwich concrete. f_{yi} = yield strength of inner steel tube and A_{so}, A_{si} and A_c = area of outer steel tube, inner steel tube, and sandwich concrete, respectively.

The value f_{scy} of the CFST specimens is determined using the formulas given by MOHURD 2014 [23], as shown:

$$f_{scy}/f_c = 1.212 + B\xi + C\xi^2 \quad (5)$$

$$B = m_1 f_y/213 + n_1 \quad (6)$$

$$C = m_2 f_c/14.4 + n_2 \quad (7)$$

The strengths of the steel tubes and the core of the concrete were connected to the values of B and C, respectively. The hexagonal specimens lacked the proper characteristics. For the octagonal CFST (which resembles a hexagonal section), the values of m_1, n_1, m_2, and n_2, were 0.140, 0.778, −0.070, and 0.026, respectively.

The equation given by Han et al. [34] to calculate f_{scy} are given as shown:

$$f_{scy}/f_c = C_1\chi^2 f_{yo}/f_c + C_2(1.14 + 0.02\xi) \quad (8)$$

$$C_1 = \alpha/(1+\alpha) \quad (9)$$

$$C_2 = (1+a_n)/(1+\alpha) \quad (10)$$

$$\alpha = A_{so}/A_c \quad (11)$$

$$a_n = A_{so}/A_{ce} \quad (12)$$

Shen et al. [22] presented modified expressions based on Eqs. recommended by MOHURD 2014 [23]. The modified Eqs. are shown below:

$$f_{scy}/f_c = a_o + B\xi + C\xi^2 \quad (13)$$

$$B = a_1(1 + b_1\chi + c_1\chi^2)(1 + df_{yo}/213) \quad (14)$$

$$C = a_2(1 + b_2\chi + c_2\chi^2)(1 + ef_c/14.4) \quad (15)$$

The parametric results of the HCFDST, HMCFDST, and S-HMCFDST columns, respectively, were used to perform nonlinear modeling. In Table 6, a summary of each parameter value was provided.

Hassanein et al. [18] provided a novel equation to design regular hexagonal CFST short columns in compression to predict the ultimate axial strength of hexagonal concrete-filled steel tubular short columns. The formula was created to enhance the predictions of the models presented by Yu et al. [19], EN 1994-1-1 [35], and those that Xu et al. [15], Ding et al. [21], respectively. Over the whole range of D/t ratios, the equation offered more dependable and accurate predictions than the other models. Below is the suggested design model for compressed hexagonal CFST short columns:

$$P_{ul,Sug} = (\gamma_c f_c' + 4.1 \times f_{rp})A_c + f_y A_s \quad (16)$$

In which γ_c represents the reduction factor which is proposed by Liang [35] as shown:

$$\gamma_c = 1.85D_c^{-0.135}\ (0.85 \le \gamma_c \le 1.0) \quad (17)$$

Table 6. Results of nonlinear fitting

Factors	HCFDST
a_o	0.918
a_1	1.045
b_1	0.232
c_1	0.646
d	−0.009
a_2	−0.004
b_2	−3.666
c_2	7.224
e	5.394

DOI: 10.21608/ERJENG.2023.201459.1168

Journal of Engineering Research (ERJ)
Vol. 7 – No. 2, 2023
©Tanta University, Faculty of Engineering
ISSN: 2356-9441 https://erjeng.journals.ekb.eg/ e ISSN: 2735-4873

Table 7. F.E results comparison of different formulae

Specimen	$N_{ul,F.E}$ (kN)	$N_{(19)}$ (kN)	$N_{(13)}$ (kN)	$N_{(5)}$ (kN)	$N_{(8)}$ (kN)	$N_{(19)}/N_{ul,F.E}$	$N_{(13)}/N_{ul,F.E}$	$N_{(5)}/N_{ul,F.E}$	$N_{(8)}/N_{ul,F.E}$
A1	787	861	805	869	900	1.094	1.023	1.104	1.144
A2	905	943	887	950	982	1.042	0.980	1.050	1.085
A3	986	1153	1017	960	1104	1.169	1.032	0.974	1.120
A4	1132	1250	1114	1057	1201	1.104	0.984	0.934	1.061
A5	1370	1393	1293	1464	1473	1.016	0.943	1.068	1.075
A6	1523	1490	1390	1561	1570	0.978	0.913	1.025	1.031
A7	1636	1786	1635	1617	1800	1.092	1.000	0.988	1.100
A8	1803	1925	1774	1755	1938	1.068	0.984	0.973	1.075
A9	2671	2887	2714	3185	3138	1.081	1.016	1.192	1.175
A10	2736	3025	2852	3324	3276	1.106	1.043	1.215	1.198
A11	2996	3153	3027	3213	3397	1.052	1.011	1.073	1.134
A12	3205	3354	3228	3414	3598	1.046	1.007	1.065	1.123
A13	943	1032	951	998	1049	1.094	1.008	1.058	1.112
A14	1098	1146	1065	1113	1163	1.043	0.970	1.013	1.059
A15	1269	1469	1250	1141	1359	1.158	0.985	0.899	1.071
A16	1502	1606	1386	1277	1496	1.069	0.923	0.850	0.996
A17	1504	1627	1481	1637	1662	1.082	0.985	1.088	1.105
A18	1632	1763	1617	1773	1798	1.081	0.991	1.087	1.102
A19	2109	2249	2007	1928	2204	1.066	0.951	0.914	1.045
A20	2252	2442	2201	2122	2397	1.084	0.977	0.942	1.064
A21	2960	3333	3051	3508	3475	1.126	1.031	1.185	1.174
A22	3208	3527	3245	3701	3668	1.099	1.011	1.154	1.143
A23	3680	3820	3589	3702	3990	1.038	0.975	1.006	1.084
A24	3912	4101	3871	3983	4271	1.048	0.990	1.018	1.092

Table 8: Mean and variation coefficient of the design models

Indices	$N_{(19)}/N_{ul,F.E}$	$N_{(13)}/N_{ul,F.E}$	$N_{(5)}/N_{ul,F.E}$	$N_{(8)}/N_{ul,F.E}$
Mean	1.077	0.989	1.037	1.099
COV	0.039	0.033	0.091	0.043

For a hexagonal section, D_c is calculated as $(D - 2t)$, where t is the steel tube thickness, D is shown in Fig. 2, f_y is the steel tube yield strength, A_s is the area of the steel tube, and A_c is the area of the infill concrete, respectively.

According to Liang and Fragomeni [36], f_{rp} is the lateral confining pressure on the concrete and f_c is the unconfined concrete cylinder strength. The confinement pressure of a regular hexagonal CFST with θ =120° was proposed by Ding et al. [20] and is depicted below:

$$f_{rp} = \begin{cases} \left(0.0491703 - 0.0007943\dfrac{B+D}{2t}\right) f_{sy} & for\ 17 \le \dfrac{B+D}{2t} < 63 \\ \left(0.0065311 - 0.0000044\dfrac{B+D}{2t}\right) f_{sy} & for\ 63 \le \dfrac{B+D}{2t} < 103 \end{cases} \quad (18)$$

Fig. 2 defines. B and D. This paper presented a modified equation of (16) to design regular HCFDST short column in compression by adding the inner tube part ($f_{yi}A_{si}$) as proposed as:

$$P_{ul,Prop} = (\gamma_c f_c' + 4.1 \times f_{rp})A_c + f_{yo}\,A_{so} + f_{yi}\,A_{si} \quad (19)$$

where f_{yi}, f_{yo} are the yield strength of inner and outer steel tubes, respectively, A_{so}, A_{si} and A_c represent the areas of outer steel tube، inner steel tube and sandwich concrete, respectively. γ_c is the reduction factor, D_c is computed as $(D - 2t - d_i)$ where d_i is the inner steel tube diameter, t is the steel tube thickness and D is illustrated in Fig. 2.

VI. COMPARISONS OF FINITE ELEMENT WITH DIFFERENT FORMULAE

Table 7 summarized the prediction results of different formulae. Table 8 illustrated the average and coefficient of variation (COV) of different formulae. For (19), the average and the coefficient of variation of the prediction value to the F.E. result ($N_{(19)}/N_{ul,FE}$) were 1.077 and 0.039, respectively, which was similar to Eq. (16) and better than (13) and (5). This indicated that (19), proposed in this paper is acceptable for the calculation of the maximum load strength of HCFDST.

VII. CONCLUSIONS

The behavior of the composite hexagonal columns with double skins and concrete filling is discussed in this research. In order to analyze and model the fundamental behavior of HCFDST columns under compression, a total of 108 columns were initially studied. The inner tube diameter-to-thickness ratio, the hollow ratio, and the steel yield stress were the parameters taken into account in the parametric analysis. The axial capacity of HCFDST short columns is significantly enhanced by raising the steel yield strength. The ultimate strength only slightly improved, by around 17% and 8%, respectively, when the inner tube thickness was increased from 3 mm to 5 mm and from 5 to 7 mm. When the hollow ratio (χ) increased from (0.48 to 0.57), (0.41 to 0.61), and (0.39 to 0.56), respectively, the ultimate load capacity increased by approximately 25%, 18%, and 17%. This was accomplished by increasing the inner tube diameter and inner tube thickness while keeping the outer tube diameter and inner tube thickness constant. For typical HCFDST short columns in compression, a new formula to calculate ultimate load has been proposed

DOI: 10.21608/ERJENG.2023.201459.1168

Journal of Engineering Research (ERJ)
Vol. 7 – No. 2, 2023
©Tanta University, Faculty of Engineering
ISSN: 2356-9441 https://erjeng.journals.ekb.eg/ e ISSN: 2735-4873

Funding: The authors state that this research has not received any type of funding.

Conflicts of Interest: The authors declare there is no conflict of interest.

REFERENCES

[1] Shosuke M., Mizuaki U., and Ikuo Y., "Concrete-filled steel tube column system-its advantages", Steel Structures, pp 33-44, 2001.
[2] Chitawadagi M.V., Narasimhan M.C., and Kulkarni S.M., "Axial strength of circular concrete-filled steel tube columns – DOE approach", Journal of Constructional Steel Research, 66(10), pp 1248–1260, 2010.
[3] Mabrouk R., Awad M., Abdelkader N. amd Kassem M., "Strengthening of reinforced concrete short columns using ferrocement under axial loading", Journal of Engineering Research, 6(3), pp 32-48, 2022.
[4] Han L-H., Wei L., and Bjorhovde R., "Developments and advanced applications of concrete-filled steel tubular (CFST) structures: members", Journal of Constructional Steel Research, 100, pp 211–228, 2014.
[5] Qing Q.L., "Nonlinear analysis of circular double-skin concrete-filled steel tubular columns under axial compression", Engineering Structures, 131, pp 639–650, 2017.
[6] Zhao X-L. and Han L-H., "Double skin composite construction", Progress in Structural Engineering and Materials, 8(3), pp 93–102, 2006.
[7] Yan X-F, Zhao Y-G. "Experimental and numerical studies of circular sandwiched concrete axially loaded CFDST short columns", Engineering Structures, 230, pp 111617, 2021.
[8] Yan X-F, Zhao Y-G. "Compressive strength of axially loaded circular concrete-filled double-skin steel tubular short columns", Journal of Constructional Steel Research, 170, pp 106-114, 2020.
[9] Tomlinson M., Chapman M., Wright H., Tomlinson A., and Jefferson A., "Shell composite construction for shallow draft immersed tube tunnels", ICE International Conference on Immersed Tube Tunnel Techniques, Manchester, UK, 1989.
[10] "Junchang C., Hong J., Mizan A., Shicai C., Daxing Z., and Liqun H., Experimental and numerical analysis of circular concrete-filled double steel tubular stub columns with inner square hollow section", Engineering Structures, 227, pp 111400, 2021.
[11] Zhao X-L., and Raphael G., "Strength and ductility of concrete filled double skin (SHS inner and SHS outer) tubes", Thin-Walled Structures, 40(2), pp 199-213, 2002.
[12] Elchalakani M., Zhao X-L., and Raphael G., "Tests of concrete filled double skin (CHS outer and SHS inner) composite short columns under axial compression", Thin-Walled Structures, 40(5), pp 415–441, 2002.
[13] Wei S., Mau S., Vipulanandan C., and Mantrala S., "Performance of new sandwich tube under axial loading: analysis", Journal of Structural Engineering, 121(12), pp 1815–1821, 1995.
[14] Sugimoto M., Yokota S., Sonoda K., and Yagishita F., "A basic consideration on double skin tube–concrete composite columns", Osaka City University and Monash University Joint Seminar on Composite Tubular Structures, Osaka, 1997.
[15] Xu W., Han L-H. and Li W., "Performance of Hexagonal CFST Members under Axial Compression and Bending", Journal of Constructional Steel Research, 123, pp 162-175, 2016.
[16] Zhang, Y-B., Han L-H, Zhou K., and Yang S. T., "Mechanical performance of hexagonal multi-cell concrete-filled steel tubular (CFST) stub columns under axial compression" Thin-Walled Structures, 134, pp 71–83, 2019.
[17] Ayough P., Ibrahim Z., Sulong N.H.R. and Hsiao P-C, "The effects of cross-sectional shapes on the axial performance of concrete-filled steel tube columns", Journal of Constructional Steel Research, 176, 2021.
[18] Hassanein M.F., Patel V.I. and Bock M., "Behaviour and design of hexagonal concrete-filled steel tubular short columns under axial compression", Engineering Structures, 153, pp 732-748, 2017.
[19] Yu M., Zha X., Ye J. and Li Y., "A unified formulation for circle and polygon concrete filled steel tube columns under axial compression". Engineering Structures,49, pp 1-10, 2013.
[20] Evirgen, B., Tuncan, A. and Taskin, K., "Structural Behaviour of Concrete Filled Steel Tubular Sections (CFT/CFST) under Axial Compression", Thin-Walled Structures, 80, pp 46-56, 2014.
[21] Ding F-X., Li Z., Cheng S. and Yu Z-W., "Composite action of hexagonal concrete-filled steel tubular stub columns under axial loading" Thin-Walled Structure, 107, pp 502–513, 2016.
[22] Shen L., Yang B., Ding M., Chen F., Alqawzai S., Elchalakani M. and Chen K., "Experimental study on the behavior of a novel stiffened hexagonal CFDST stub column under axial load", Journal of Structural Engineering, 148(1), 2022.
[23] MOHURD (Ministry of Housing and Urban-Rural Development of the People's Republic of China). Technical code for concrete filled steel tubular structures. GB 50936-2014. Beijing: MOHURD, 2014.
[24] ABAQUS Standard, User's Manual. The Abaqus software is a product of Dassault Systèmes Simulia Corp., Providence, RI, USA Dassault Systèmes, Version 6.14, USA., 2014.
[25] Elchalakani M., Karrech A., Hassanein M.F. and Yang B., "Plastic and yield slenderness limits for circular concrete filled tubes subjected to static pure bending", Thin-Walled Structure, 109, pp 50-64, 2016.
[26] Dai X. and Lam D., "Numerical modelling of the axial compressive behaviour of short concrete-filled elliptical steel columns", Journal of Constructional Steel Research, 66(7), pp 931–942, 2010.
[27] Dai X., Lam D., Jamaluddin N, Ye J., "Numerical analysis of slender elliptical concrete filled columns under axial compression", Thin-Walled Structure, 77, pp 26–35, 2014.
[28] Hassanein M.F., Patel V.I., "Round-ended rectangular concrete-filled steel tubular short columns: FE investigation under axial compression", Journal of Constructional Steel Research, 140, pp 222–236, 2018.
[29] Pagoulatou M., Sheehan T., Dai X. and Lam D, "Finite element analysis on the capacity of circular concrete-filled double-skin steel tubular (CFDST) stub columns", Engineering Structure, 72(1), pp 102–112, 2014.
[30] Anumolu S., Abdelkarim O. and El-Gawady M., "Behavior of hollow-core steel-concrete-steel columns subjected to torsion loading", Journal of Bridge Engineering.,21 (10), 2016.
[31] Ottosen N. and Ristinmaa M., 2005. "The mechanics of constitutive modeling", Elsevier, 2005.
[32] ACI (American Concrete Institute), Building code requirements for structural concrete and commentary. ACI 318. Chicago: ACI, 2014.
[33] Bazant Z.and Emilie B-G., "Statistical prediction of fracture parameters of concrete and implications for choice of testing standard." Cement and Concrete Research, 32 (4), pp 529–556, 2002.
[34] Han L-H., Dennis L., and Nethercot D. A., "Design guide for concrete filled double skin steel tubular structures", Boca Raton, FL: CRC Press/ Taylor & Francis Group, 2019.
[35] EN 1994-1-1: Eurocode 4. Design of composite steel and concrete structures. Part 1. 1, General rules and rules for buildings. European Committee for Standardization, 2004.
[36] Liang QQ., "Performance-based analysis of concrete-filled steel tubular beam columns", Part I: Theory and algorithms, Journal of Constructional Steel Research, 65(2), pp 363–73, 2009.

DOI: 10.21608/ERJENG.2023.201459.1168